



A mathematical representation of the reactive scope model

Justin Wright^{1,2} · Kelly Buch³ · Ursula K. Beattie⁴ · Brenna M. G. Gormally⁴ · L. Michael Romero⁴ · Nina Fefferman^{1,2}

Received: 13 December 2022 / Revised: 15 May 2023 / Accepted: 9 August 2023
© The Author(s) 2023

Abstract

Researchers have long sought to understand and predict an animal's response to stressful stimuli. Since the introduction of the concept of homeostasis, a variety of model frameworks have been proposed to describe what is necessary for an animal to remain within this stable physiological state and the ramifications of leaving it. Romero et al. (Horm Behav 55(3):375–389, 2009) introduced the reactive scope model to provide a novel conceptual framework for the stress response that assumes an animal's ability to tolerate a stressful stimulus may degrade over time in response to the stimulus. We provide a mathematical formulation for the reactive scope model using a system of ordinary differential equations and show that this model is capable of recreating existing experimental data. We also provide an experimental method that may be used to verify the model as well as several potential additions to the model. If future experimentation provides the necessary data to estimate the model's parameters, the model presented here may be used to make quantitative predictions about physiological mediator levels during a stress response and predict the onset of homeostatic overload.

Keywords Reactive scope · Stress · Stress schedule · Homeostasis · Senescence

Mathematics Subject Classification 92C30

1 Introduction

According to Levine (2005), references to the idea of *homeostasis* and its disruption, which is often referred to now as *stress*, can be traced at least as far back as early Greek physicians and our modern perspectives on stress can largely be traced back to Cannon (1932) and Selye (1946). Attempts to provide a well-defined and widely-accepted definition for stress in animals have been ongoing for nearly as long with much of the

Justin Wright and Kelly Buch contributed equally to this work.

Extended author information available on the last page of the article

ambiguity coming from the cyclical nature of defining a stimulus as stressor if it elicits a stress response and a stress response as a physiological or behavioral response to a stressor (Levine 2005; Romero et al. 2009). More recently, Sterling and Eyer (1988) proposed the allostasis model in an effort to redefine the concept of stress in terms of energy acquisition and usage. In turn, McEwen and Wingfield (2003) used the concept of allostasis to explain physiological mediator levels, such as glucocorticosteroids, through ecological factors like foraging success, bad weather, and habitat changes.

Romero et al. (2009) introduced the reactive scope model to both further the allostasis model while also addressing its weaknesses. Unlike the allostasis model, which focuses heavily on resource allocation and expenditure, the reactive scope model allows the concept of stress or a stress event to be broadly interpreted allowing for the consideration of changes to homeostasis or even anticipation of changes to homeostasis. Broadly speaking, the reactive scope model introduces two novel components to the consideration of stress. First, the concept of a *stressor* or *stress event*, a stimulus which causes stress, is allowed to include responses in anticipation of an environmental stressor. Second is the addition of the eponymous *reactive homeostasis* range to the traditional homeostasis model. The reactive homeostasis range is believed to exist as a dynamic buffer zone representing temporary resilience between traditional homeostasis and homeostatic overload which shrinks, temporarily or permanently, when an animal is experiencing a stress event causing mediator levels outside of homeostasis. The authors use the term “wear and tear” to refer to the shrinking of the reactive homeostasis range due to the accumulated cost of maintaining the stress response. The authors also point out that the use of “wear and tear” should not be, in this case, associated with the slow accumulation of damage and aging.

Since the introduction of the reactive scope model, many studies have interpreted results in terms of the model (Aguilar et al. 2016; Beattie et al. 2023a; Charpentier et al. 2018; Crespi et al. 2013; Eguizábal et al. 2022; Gabriel et al. 2018; Houtz et al. 2022; Howell and Sanchez 2011; Leishman et al. 2022; Lima et al. 2022; Pahuja and Narayan 2021; Roast et al. 2019; Romero 2012; Schoenle et al. 2018 to name a few). On the other hand, a relative few studies, including Gormally et al. (2019b), Beattie et al. (2023b), Gormally et al. (2019a), DuRant et al. (2016b), and DuRant et al. (2016a) have set out with the specific goal of verifying the reactive scope model with varying degrees of success. Generally, these studies caused stress reactions in groups of wild-caught birds, allowed the groups to recover for varying lengths of time, then induced new stress reactions with the hypothesis that groups with longer recovery times would have enough time to recover from reactive homeostasis allowing for a reduced stress response in comparison to groups with shorter recovery times. However, since the current version of the reactive scope model is purely conceptual, there was no way for these researchers to determine the necessary duration of stress events or recovery to ensure the hypothesized wear and tear would be observable.

As Grindstaff et al. (2022), Servedio et al. (2014), and Zavala et al. (2019) have pointed out, mathematical models can be powerful tool in the investigation theoretical biological and endocrinological theory. In Luttbeg et al. (2021), Taborsky et al. (2021), and Taborsky et al. (2022), the authors have used mathematical models to explore the evolution of the stress response and how repair rates influence basal levels. Mathematical frameworks and models are already being utilized in other investigations of

the hypo-pituitary-adrenal (HPA) axis, stress, and the stress response. Using mathematical models to investigate the HPA axis itself has garnered a great deal of interest since the seminal work provided by Dempsher et al. (1984). Reviews of the subject have been offered by Lightman (2008), Goel et al. (2014), Nicolaides et al. (2017), Tsigos and Chrousos (2002), Lightman and Conway-Campbell (2010), Vinther et al. (2011), Gudmand-Hoeyer et al. (2014), Spiga et al. (2015), Zavala et al. (2019) and Hosseinichimeh et al. (2015). Hosseinichimeh et al. (2015) in particular offers a comparison of 14 published models and attempts to fit them to data with varying results and then goes on to provide an updated form of the most promising model. Since these reviews, others, such as Rao and Androulakis (2019) and Stanojević et al. (2018), have continued efforts to explore these models and discuss progress. The models constructed thus far have sought to capture the complex nature of the HPA axis made up of a system of molecular interactions, reaction-transport processes, and pathways using either systems of ordinary differential equations or delay differential equations that describe both basal and stress induces cortisol levels in humans or corticosterone levels in rats. However, as Stanojević et al. (2018) points out, while the field of mathematical modeling of the HPA axis is rich and growing, “there is still neither consensus nor a common representation of the core feedback mechanisms.” In addition, the models have often been constructed and calibrated with particular data sets and the models’ predictions are not tested across other published data sets. Further, while the analysis of these models has included in silico experimentation with acute stress events that perturb the system being described, they have not explored the degradation of the system’s ability to cope with prolonged or severe stress. These models may also have little to no application outside of the species for which they were designed and the molecules involved in the stress response process may differ among species (Taborsky et al. 2021). Finally, while existing models of the HPA axis are simplifications of the complex system, they are potentially unapproachable to researchers whose backgrounds do not include a significant amount of mathematics (Fawcett and Higginson 2012).

One weakness of the reactive scope model in its current formulation is that it is a conceptual framework presented graphically. That is, to date there has been no quantitative representation of the reactive scope model provided. As a consequence, there has been no way to predict experimental outcomes leaving no way to objectively verify the model. As pointed in by Grindstaff et al. (2022), the formulation of a mathematical model cannot, on its own, verify the reactive scope model. Confirming the conceptual model will require the combined work of empiricists and mechanistic models like the one presented here. With a mathematical model describing the reactive scope model, the parameters of the mathematical model can be estimated using regression techniques and experimental data, then the model may be used to predict physiological mediator levels in particular circumstances and this prediction can in turn be compared to experimental data. If the model and data are found to be in good agreement, we may presume that the mathematical model accurately captures the stress response process. If not, then the model can be adjusted as needed.

We provide a quantitative framework for the reactive scope model as well as several of its components. We begin describing general stress events and representing those stress events mathematically as a function of time in Sect. 2.1. In Sect. 2.2 we provide a time-dependent form for mediator levels subject to circadian and seasonal variation and

then describe the reactive scope model as a system of ordinary differential equations that describe the boundaries between the ranges in the reactive scope model. We proceed then to provide several examples of the flexibility of this mathematical model. In Sect. 3 we use the mathematical model to duplicate the results of an empirical study and provide a broad analysis of the mathematical model. We provide a method to determine the veracity of the model empirically in Sect. 4. Finally, in Sect. 5.1, we provide several possible additions to the reactive scope model and discuss its weaknesses.

2 The model

Fischer and Romero (2013), McEwen (2003), McEwen and Wingfield (2003), and Romero et al. (2009) all seek to describe the effects of stress on physiological mediators such as glucocorticoids, antibody titers, catecholamines, and heart rate to name a few. In the reactive scope model, Romero et al. (2009) hypothesized that a physiological mediator, such as changes in behavior, mediators of immune function, and mediators of the HPA axis as presented by McEwen (2003) and McEwen and Wingfield (2003), to be in one of four classifications based on range: predictive homeostasis, reactive homeostasis, homeostatic overload, and homeostatic failure. We adopt the same terminology here. Mediator values are in the *predictive homeostasis* range when an animal is able compensate for any normal fluctuations caused by seasonal and circadian changes as well as normal foraging behavior as might be associated with allostasis. Romero et al. (2009) introduced the *reactive homeostasis* range. Mediator values in the reactive homeostasis range are beyond the normal fluctuations represented by the predictive homeostasis range but are still low enough to temporarily avoid entering homeostatic overload. The terms predictive homeostasis and reactive homeostasis are borrowed from Moore-Ede (1986) and together they represent the normal reactive scope for an animal. Mediator levels that exceed the reactive homeostasis range are said to be in the *homeostatic overload* range and will induce a pathological state. The final range, *homeostatic failure*, is depicted by Romero et al. (2009) as below the predictive homeostasis range and represents an animal's inability to maintain or regulate normal mediator levels and death follows rapidly. A graphical representation of the reactive scope model in the absence of stress events is presented in Fig. 1 where the thresholds between the predictive homeostasis range, reactive homeostasis range, and homeostatic overload range are labeled $P(t)$ and $R(t)$ respectively. See Sect. 2.2 for further discussion of these values.

An important aspect of the reactive scope model is wear and tear: the sizes of the ranges associated with each classification can change temporarily or permanently in response to stress events. “Sizes” refers to the distance between the threshold values between the ranges on the mediator y -axis. The result of this wear and tear is that a raised mediator level can be tolerated by an animal for some period of time before homeostatic overload is induced, mimicking resilience, and that the same stress response may lead to homeostatic overload more rapidly in the future. According to Romero et al. (2009), “there are two ways to enter Homeostatic Overload: the concentration or level of the mediator extends beyond the normal reactive scope; or the

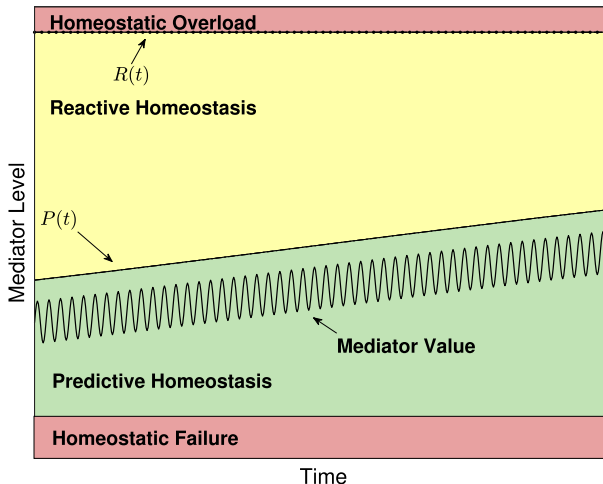


Fig. 1 A generic example of mediator levels in the reactive scope model and of the system in (8) with no stress event used to duplicate figures depicting reactive scope given by Romero et al. (2009). Note that the size of the reactive homeostasis range (the distance between $R(t)$ and $P(t)$) is shrinking due to a long-term, seasonal variation in the size of the predictive homeostasis range. The fluctuations in the mediator value are meant to mimic circadian variation

concentration or level of the mediator remains in the Reactive Homeostasis range for an extended period.”

We introduce our model below by first discussing and giving a mathematical representation of stress events and schedules and then of the thresholds between three primary characteristic ranges of the reactive scope model.

2.1 The stress schedule

Romero et al. (2009) defines a stress event as an unpredictable event in an animal’s environment and that a stress response is a physiological reaction to the event. They emphasize the exact behavior of the stress response is dependent on the mediator or behavior in question. Further, a stress event or response can have a variety of causes including allostatic overload as described by McEwen and Wingfield (2003), predation, or may even be the anticipation of a stressor event. Here, we disregard the distinction between a stimulus event and a response and use the term *stress event* to refer to any change in a physiological mediator level regardless of whether the cause is an environmental stimulus, allostatic overload, or psychological cause. To describe a mediator level during a stress event or series of stress events, we use the *stress schedule* as described by

$$s(t) = \sum_{i=1}^n s_i \psi_{\mu_i, \sigma_i}(t) \quad (1)$$

where n is the number of stress events being considered, s_i is the magnitude of the stress response for the i^{th} stress event, ψ_{μ_i, σ_i} is a function that captures the desired

behavior of the stress event (e.g. up- and down-regulation time, increase and decrease rates, etc.), and μ and σ are parameters that dictate the time and duration of the event. It should be noted that different mediators will respond differently in any given situation and that a stress event and subsequent stress schedule are meant to capture the behavior of a single mediator over time. Thus, if several mediators are being considered, their respective stress schedules should be plotted on separate axes.

We provide three possible forms for ψ_{μ_i, σ_i} below and their graphs are shown in Fig. 2. First, the graphical model provided by Romero et al. (2009) describes stress events that are best presented using

$$\psi_{\mu_i, \sigma_i}(x) = \begin{cases} 1 & \mu_i < x < \mu_i + \sigma_i \\ 0 & \text{otherwise} \end{cases} \quad (2)$$

where μ_i and σ_i are strictly positive constants. Here, μ_i would represent the beginning of the i^{th} stress event and σ_i indicates the duration of the event. This form of ψ_{μ_i, σ_i} is useful for demonstrative purposes but is likely to provide an oversimplified representation of the stress response as it will result in mediator levels up- and down-regulating instantaneously.

Rich and Romero (2005) recorded corticosterone levels in birds undergoing induced stress. The data presented suggests that a stress response commences at the initiation of a stress event and is up-regulated throughout the stress event. At the conclusion of the stress event, the mediator is down-regulated over a period of time that is longer than the stress event. Such a process is better represented using ψ_{μ_i, σ_i} given by

$$\psi_{\mu_i, \sigma_i} = \begin{cases} \frac{1}{\sigma_i}(x - \mu_i) & \mu_i < x < \mu_i + \sigma_i \\ \frac{1}{\sigma_i - \alpha\sigma_i}(t - \mu_i - \sigma_i) & \mu_i + \sigma_i < x < \mu_i + \alpha_i\sigma_i \end{cases} \quad (3)$$

where $\alpha > 0$ and $\alpha \neq 1$. The value of μ_i should coincide with the beginning of the i^{th} stress event (or can be adjusted if the delay period between the stimulus and response is known) and σ_i represents the duration of the stress event or up-regulation period. The parameter α represents how much longer down-regulation of the mediator takes. For example, Rich and Romero (2005) showed that the down-regulation of CORT is 3 to 4 times as long as the up-regulation.

Other options may be more appropriate for the ψ depending on circumstances. For example,

$$\psi(x) = e^{-\left(\frac{t-\mu_i}{\sigma_i}\right)^2} \quad (4)$$

where μ_i represents the mid-time of the stress event would provide a continuously differentiable version of the stress event that may more accurately capture the nature of the up- and down-regulation. However, σ_i in Eq. (4) does not directly represent the duration of the stress event nor response. That is, larger values of σ_i would imply a longer duration but neither the event nor the response would have a duration equal to σ_i . Figure 2 compares the three descriptions for stress events provided here.

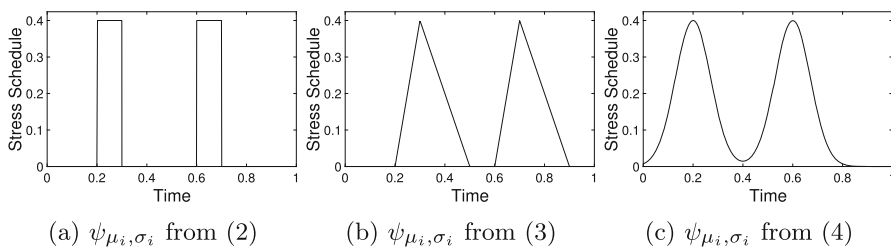


Fig. 2 (a) The form of the stress schedule is given in (2). Stress schedules where $s_1 = s_2 = 0.4$, $\sigma_1 = \sigma_2 = 0.1$, $\mu_1 = 0.2$, and $\mu_2 = 0.6$ using different forms for ψ . These schedules are presented independently from consideration of physiological mediator, so the values on the independent axis are meaningless here. **b** With $\alpha = 3$. Note that each event starts at the appropriate μ value. **c** The value of μ denotes the mid-time of the event

2.2 Wear and tear of the reactive scope

A defining feature of the reactive scope model is what (Romero et al. 2009) referred to as “wear and tear.” Unlike the use of “wear and tear” to refer to the long-term, slow accumulation of damage and aging (McEwen 1998), wear and tear is the idea that repeated or prolonged stress responses may cause a decrease in the size of an animal’s reactive homeostasis range during the stress response, thereby making it possible for future stress events of the same magnitude to lead to homeostatic overload. We model this behavior by changing the threshold curves between the characteristic ranges of the reactive scope model.

As the reactive scope model undergoes change in response to physiological mediator levels, we begin by describing the mediator level under consideration at time t by $y(t)$ where

$$y(t) = a_s \sin(b_s t) + a_c \sin(b_c t) + s(t) + y_c, \quad (5)$$

a_s and a_c are amplitude the of seasonal and circadian variation respectively, b_s and b_c are period of seasonal and circadian variation respectively, y_c is the basal level of the physiological mediator (and must be chosen large enough to ensure that $y(t)$ is nonnegative), and $s(t)$ is the stress schedule as defined in (1). Thus, the mediator level $y(t)$ is driven both physiological factors and the stress schedule.

Next, we describe the initial threshold curve, $P(t)$, between the predictive homeostasis range and reactive homeostasis range by

$$P(t) = a_s \sin(b_s t) + a_c + y_c + y_{act} \quad (6)$$

where a_s , b_s , a_c , y_c are as above and y_{act} represents changes in mediator level due to predictable activity.

We then denote the boundary between reactive homeostasis and homeostatic overload by $R(t)$ and describe the hypothesized wear and tear of the reactive scope range by allowing $R(t)$ to change in response to $y(t)$. Since the reactive scope model assumes that the reactive scope range will return to its pre-stimulus size if the stress event fails to induce homeostatic overload, we introduce a new quantity, $M(t)$, to represent the maximum value that $R(t)$ can recover to at the conclusion of a stress event. According

to Romero et al. (2009) with our notation, $R(t) \leq M(t)$ for all t , $R(t)$ should decrease temporarily if $P(t) < y(t) < R(t)$, should decrease permanently if $y(t) > R(t)$, and increases to $M(t)$ when $y(t) < P(t)$. Further, $M(t)$ decreases permanently when $y(t) > R(t)$. We let $\theta(x)$ denote the Heaviside function

$$\theta(x) = \begin{cases} 0 & x \leq 0 \\ 1 & x > 0 \end{cases}. \quad (7)$$

Then,

$$\begin{aligned} \frac{dM}{dt} &= -r_1\theta(y(t) - R(t)) \\ \frac{dR}{dt} &= -r_2\theta(y(t) - P(t)) + r_3\theta(P(t) - y(t))\theta(M(t) - R(t)) \end{aligned} \quad (8)$$

where $M(0) = R(0) = M_0$; r_1 , r_2 , and r_3 are all strictly positive; and $r_1 \leq r_2$. The system given in (8) mimics figures given by Romero et al. (2009) by letting $r_1 = r_2 = r_3$ as is shown in Fig. 1. In the absence of a stress event, $M(t) = R(t)$ for all t -values and their curves overlap. Here, $a_s = 0.24$, $a_c = 0.02$, $y_c = 0.3$, $y_{act} = 0.01$. Note that the homeostatic failure range would appear below the predictive homeostasis range but is omitted in subsequent figures for simplicity. For the sake of this work, we assume $r_1 = r_2 = r_3$ unless otherwise specified. In Sect. 5.1 we provide several possible additions to the base model presented here and focus on the characteristics of the basic model for now.

To demonstrate the characteristics of the model, we consider a few examples independent from any particular experiment or mediator level. We set independent axes to scale from 0 to 1 where 1 can be thought of as the level of maximal effect (similar to C_{100} in pharmacology (Derendorf et al. 2020)). Similarly, dependent axes are scaled to 1 to indicate experiment duration and we continue this convention unless otherwise noted. Figure 3 shows several representations of the reactive scope model along with various choices of ψ_{μ_i, σ_i} . For each choice of ψ_{μ_i, σ_i} , the length of time for which $y(t) > P(t)$ is different resulting in different behaviors in $R(t)$. Since $y(t) < R(t)$ for all t in each graph, $M(t) = M_0$ for each graph.

For Fig. 3, and all remaining depictions of the model, the homeostatic failure range is removed to focus on the relevant portions of the figures. Further, with the exception of the figures in Sect. 3, figures throughout this work are meant to depict the qualitative relationships between an arbitrary physiological mediator and the homeostatic overload (red) and reactive homeostasis (yellow) ranges. As such, the scaling of the axis is effectively arbitrary and irrelevant.

Figure 4 shows reactive scope along with mediators driven by a stress schedule with two stress events. Since the first stress event does not cause homeostatic overload, the value of $R(t)$ is temporarily decreased but $M(t)$ does not. Thus, $R(t)$ recovers to the original maximum value M_0 . The second stress event lasts long enough for the reactive scope to decrease leading to homeostatic overload without the mediator level increasing further. As a result, the value of $M(t)$ decreases permanently. Thus, the threshold value $R(t)$ can never recover to the original value M_0 .

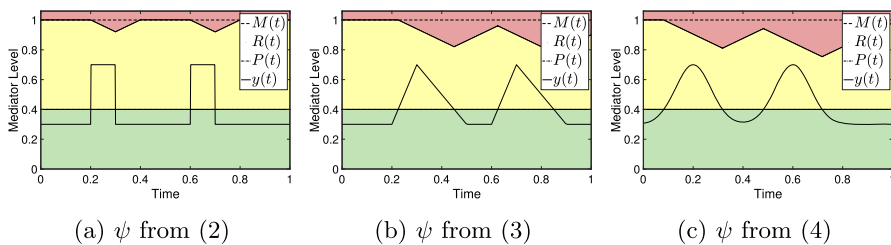


Fig. 3 Mediator levels and homeostatic ranges within the reactive scope model. Since no particular mediators are being presented, the value 1 on the dependent axis would correspond to the mediator level of maximal effect. Similarly, values on the independent axis can be viewed as a proportion of the duration of an experiment. **a–c** A stress schedule where $s_1 = s_2 = 0.4$, $\sigma_1 = \sigma_2 = 0.1$, $\mu_1 = 0.2$, and $\mu_2 = 0.6$. The ranges are colored in correspondence to those in Fig. 1. **b** with $\alpha = 3$. Note that each event starts at the appropriate μ value. **c** The value of μ denotes the mid-time of the event

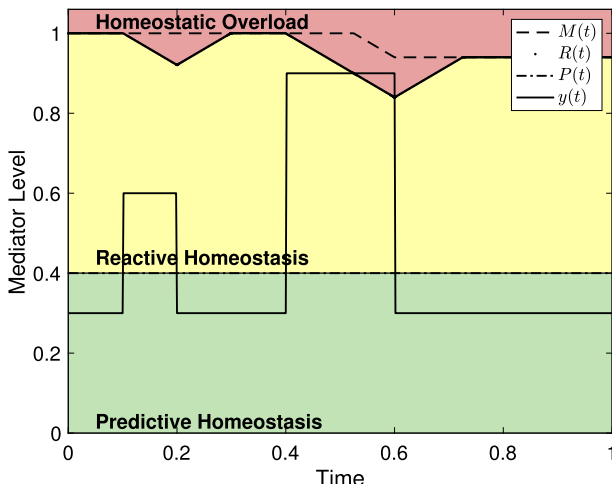


Fig. 4 The reactive scope model with mediator levels driven by a stress schedule with two stress events. Here, $s_1 = 0.3$, $\mu_1 = 0.1$, $\sigma_1 = 0.1$, $s_2 = 0.6$, $\mu_2 = 0.4$, and $\sigma_2 = 0.2$. The first stress event does not cause homeostatic overload, so the value of $M(t)$ stays fixed while $R(t)$ decreases then recovers to the value of $M(t)$. During the second stress event, the raised value of $y(t)$ causes $R(t)$ to decrease below $y(t)$ leading to homeostatic overload resulting in a permanent decrease in $M(t)$

Figure 5 shows reactive scope along with mediators driven by a stress schedule and undergoing circadian variation. The magnitude of the stress event is the same in both, but the first causes homeostatic overload because it occurs when basal levels are at their peak. As a result $M(t)$ is permanently decreased. Despite having the same magnitude, the second stress event does not cause the mediator level to grow above the predictive homeostasis range so $R(t)$ does not decrease.

3 Replication of experimental results

A number of empirical studies have interpreted results using the reactive scope model (Aguilar et al. 2016; Beattie et al. 2023a; Charpentier et al. 2018; Crespi et al. 2013;

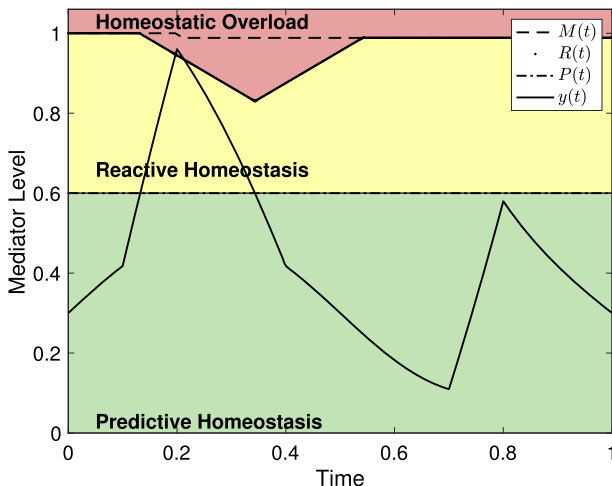


Fig. 5 Reactive scope with mediator driven by a stress schedule and circadian variation. Here $a_c = 0.2$, $b_c = 2\pi$, $y_c = 0.3$, and $y_{act} = 0.1$. For the stress schedule, $s_1 = s_2 = 0.47$, $\sigma_1 = \sigma_2 = 0.1$, $\mu_1 = 0.1$, and $\mu_2 = 0.7$. ψ_{μ_i, σ_i} is taken from (3) with $\alpha = 3$

Eguizábal et al. 2022; Gabriel et al. 2018; Houtz et al. 2022; Howell and Sanchez 2011; Leishman et al. 2022; Lima et al. 2022; Pahuja and Narayan 2021; Roast et al. 2019; Romero 2012; Schoenle et al. 2018). However, only a few studies, including Beattie et al. (2023b), Gormally et al. (2019b), Gormally et al. (2019a), DuRant et al. (2016b), and DuRant et al. (2016a), have been conducted with the explicit purpose of investigating the reactive scope model. As these studies include the use of accepted situations known to elicit a stress response, regular measurements of physiological mediators associated with the stress response, and provide ample information for the recreation of results using the model, we focus on the latter group here. The studies predominantly focus on corticosterone levels in birds. Corticosterone (CORT) is the primary avian glucocorticoid (Holmes and Phillips 1976), though catecholamines have also been found to be a valid indicator of the stress response and a good fit for the reactive scope model (Fischer and Romero 2013). We replicate some of the results related to CORT shown by DuRant et al. (2016a) in which CORT levels were measured four times over a 25 day period. Since the measurements in the study were too infrequent to capture circadian variation, we will base basal levels on those found by Breuner et al. (1999) where basal CORT levels in Gambel's White-Crowned Sparrow (*Zonotrichia leucophrys gambeli*) were found to vary daily with a maximum basal value less than 30 ng/ml occurring just before the active period. We will assume a similar pattern holds for the house sparrows (*Passer domesticus*) used by DuRant et al. (2016a). We will ignore seasonal variation due to the relatively short time period for the experiment.

To mimic the above mentioned circumstances, we set $y_c = 12$ ng/ml, $a_s = 0$ (and therefore $b_s = 0$), $a_c = 6$ ng/ml, and $b_c = 2\pi$. Figures provided by DuRant et al. (2016a) indicated that CORT levels increased from day 1 to day 12 of the experiment, then declined until day 25 which was the day of the last blood sample. Accordingly,

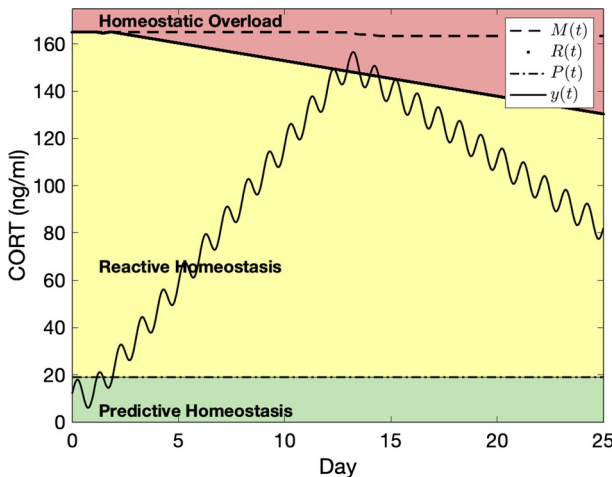


Fig. 6 A recreation of the mediator levels for birds with artificially elevated CORT levels from DuRant et al. (2016a). The oscillation is caused by the circadian variation in $y(t)$

we will use a single stress event with ψ in the form of (3) with $s_1 = 140$ ng/ml, $\mu = 1$ day, $\sigma = 11$ days. CORT levels had not returned to normal at the time of the last blood sample, so we set $\alpha = 4$ assuming the pattern presented continues.

DuRant et al. (2016a) indicated that the birds with artificially elevated CORT levels had decreased wound healing ability indicating that this group may have experienced homeostatic overload as a result of the experiment (though the authors note the results were not statistically significant). As it is not possible to estimate y_{act} , M_0 , r_1 , r_2 , and r_3 from the information given, we determine these values to be $y_{act} = 1$, $M_0 = 165$ ng/ml and $r_1 = r_2 = r_3 = 1.5$ by inspection. The model output with these variables is shown in Fig. 6.

Our goal here is not to validate nor reject the work of DuRant et al. (2016a). Neither do we claim that the ability to use the mathematical framework for reactive scope presented here to reproduce empirical work validates the mathematical formulation of the model nor the conceptual framework. Rather, we present this recreation in hopes of showing the flexibility and potential of the mathematical framework.

3.1 Analysis of the model

The reactive scope model is entirely driven by the mediator level $y(t)$ which is, in turn, driven by seasonal and circadian variation and the stress schedule. The system given in (8) predicts no change in $R(t)$ nor $M(t)$ unless $y(t) > P(t)$. That is, in the absence of stress there is no change in reactive scope. (In Sect. 5.1 we consider a version of the model that allows $R(t)$ and $M(t)$ to decrease over time.) In the presence of a stress event and elevated mediator levels, the characteristics of the mediator largely determine the behavior of the system. A simple, stationary pendulum serves as a good analogy for this system. Left alone, the pendulum will not undergo any change. If the pendulum is perturbed in some way, it will react but the characteristics of that reaction

will depend on the specifics of the force applied. Much like the pendulum, mediator levels can be manipulated in a variety of ways.

For a minor stress event, one for which the mediator level $y(t)$ only temporarily exceeds $P(t)$ and does not exceed $R(t)$, the choice of ψ_{μ_i, σ_i} has no significant impact on the predictions of the model. The system in (8) predicts that $R(t)$ will decrease while $y(t)$ exceeds $P(t)$, but that decline is in no way proportional to the magnitude of $y(t)$ nor the rate of increase of $y(t)$. Figure 7 shows the reactive scope system with stress events using different ψ_{μ_i, σ_i} and different magnitudes, but for each the the length of the time interval in which $y(t) > P(t)$ is the same. All figures in this section are given with unit-less axes that can be assumed to represent the proportion of the mediator experiment time. Thus, the model is not sensitive to the choice of ψ_{μ_i, σ_i} if homeostatic failure is never induced.

Similarly, if a stress event is significant enough for $y(t)$ to exceed $R(t)$, then only the length of the time interval during which $y(t) > R(t)$ causes $M(t)$ to decline. Two stress events with different characteristics and magnitudes will cause the same decline in $M(t)$ if the time spent with $y(t) > R(t)$ is the same. However, stress events with different characteristics will cause the mediator level to spend different amounts of time in the reactive homeostasis range leading to different declines in $R(t)$. Figure 8 shows two versions of the reactive scope model with both spending the same amount of time in homeostatic overload.

As Fig. 8 suggests, the reactive scope model places significant emphasis on the duration of a stress event. Figure 9 shows two versions of the system in (8) with stress events of different magnitude and duration. As can be seen, a severely elevated mediator level may not lead to homeostatic overload if its duration is short enough, while having mediator levels elevated to the reactive homeostasis range for a prolonged period may lead to homeostatic overload.

The rate of down-regulation of a physiological mediator may provide some insight into r_2 , the rate of decrease of $R(t)$. If an animal has a down-regulation rate that is greater than r_2 , then that animal would not be able to escape homeostatic overload once begun. Figure 10 describes such an event. This would imply that r_2 must be greater than the down-regulation rate for a given mediator.

4 Verification of the model

As the reactive scope model predicts a decline in the reactive homeostasis range during a stress response, and a decline in the maximal reactive homeostasis during a significant stress response, the model may be verified if repeated stress events induce homeostatic overload over shortened time intervals.

We consider a series of stress events that each cause a rise in $y(t)$ significant enough to induce homeostatic overload and spaced far enough apart to allow the value of $R(t)$ to recover to the value of $M(t)$ and assume that $r_1 = r_2 = r_3 = r$. See Fig. 11. For the first stress event, we let τ_1 denote the length of time during which $P(t) < y(t) < R(t)$. During this time span, $R(t)$ will decline as $y(t)$ continues to increase until their values intersect. Denote the mediator level when the curves intersect by y_1^* . Since we know that $R(t)$ decreased by $r\tau_1$ during this time interval, we know that $M_0 = y_1^* + r\tau_1$. Since

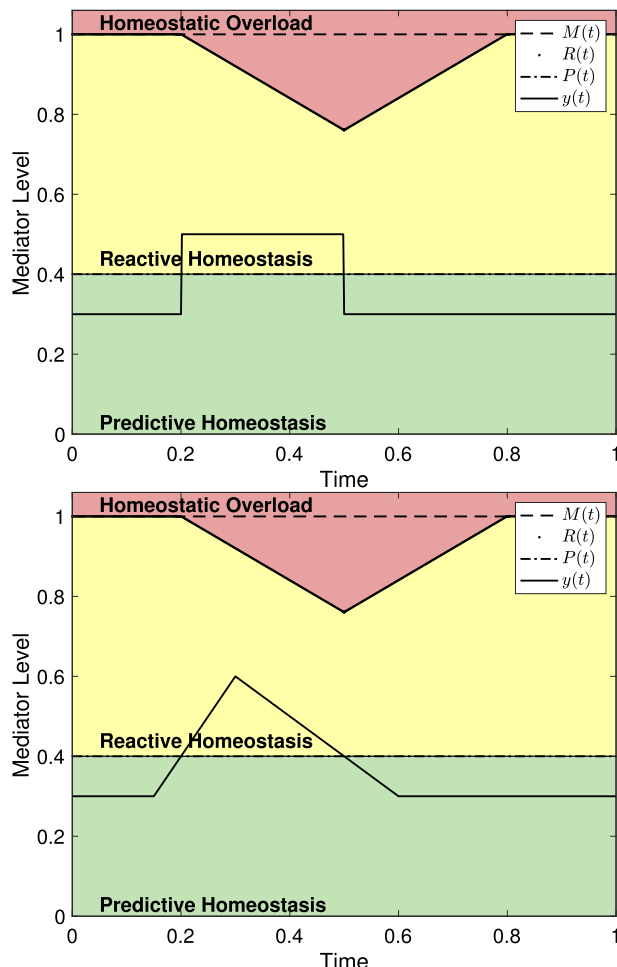


Fig. 7 Two versions of the reactive scope system as presented in (8) using different ψ_{μ_i, σ_i} functions. In both, $y(t) > P(t)$ for $0.2 < t < 0.5$ and $R(t)$ is the same for both. (left) ψ_{μ_i, σ_i} as given in (2) with $\mu = 0.2$, $\sigma = 0.3$, and $s_1 = 0.2$. (right) ψ_{μ_i, σ_i} as given in (3) with $\mu = 0.15$, $\sigma = 0.15$, and $\alpha = 3$

the first stress event induced homeostatic overload, the value of $M(t)$ will decrease. If the period of homeostatic overload is denoted by t_1 , then $M(t) = M_0 - rt_1$ at the conclusion of the period of homeostatic overload.

Similarly, during the second stress event $R(t)$ declines by $r\tau_2$ until it intersects $y(t)$ at the mediator level y_2^* and homeostatic overload commences. We denote the duration of homeostatic overload by τ_2 and note that $M(t)$ declines by $r\tau_2$ during this time. Thus, $y_2^* + r\tau_2 = M_0 - rt_1$. That is

$$M_0 = y_2^* + rt_1 + r\tau_2. \quad (9)$$

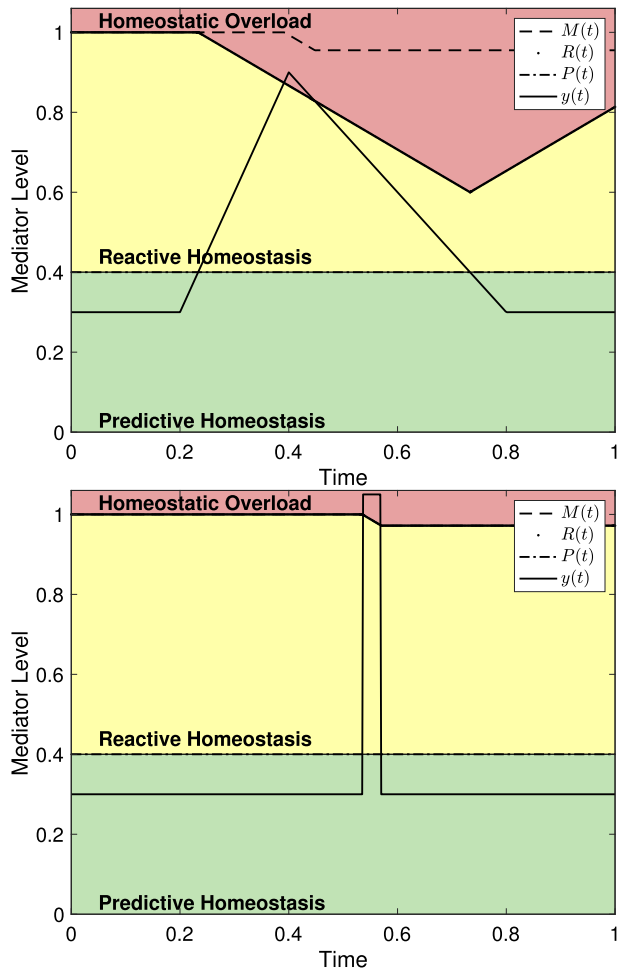


Fig. 8 Two versions of the reactive scope model with homeostatic overload. In both, $y(t) > R(t)$ for approximately 0.033834 time units and, therefore, $M(t)$ decreases by 0.033834 r_1 (with $r_1 = 0.8$ here). (left) ψ_{μ_i, σ_i} as in (3) with $s_1 = 0.6$, $\mu = 0.2$, $\sigma = 0.2$, and $\alpha = 3$. (right) ψ_{μ_i, σ_i} as in (2) with $\mu \approx 0.39474$, $\sigma \approx 0.42857$, and $s_1 = 0.75$

We know from the first stress event that $M_0 = y_1^* + r\tau_1$, thus

$$y_2^* + r\tau_2 = y_1^* + r\tau_1 - rt_1 \quad (10)$$

$$rt_1 - r\tau_1 + r\tau_2 = y_1^* - y_2^* \quad (11)$$

$$r = \frac{y_1^* - y_2^*}{t_1 - \tau_1 + \tau_2}. \quad (12)$$

Repeating this pattern for another stress event, we may find that

$$M_0 = y_3^* + rt_1 + rt_2 + rt_3. \quad (13)$$

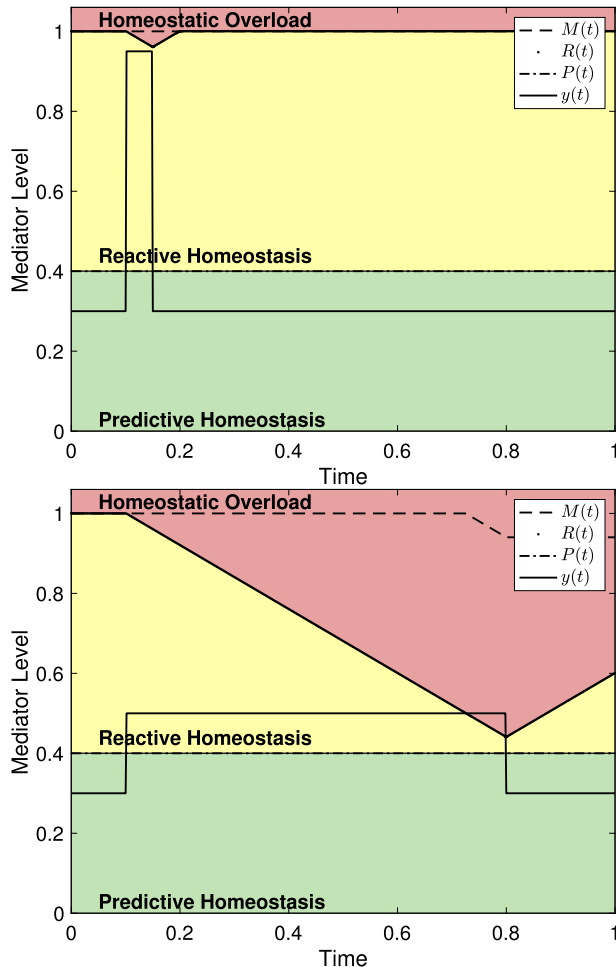


Fig. 9 The reactive scope model shown with mediator levels of varying magnitude and duration. (left) A mediator level with $s_1 = 0.65$, $\mu = 0.1$, and $\sigma = 0.05$ does not cause homeostatic overload. (right) A mediator level with $s_1 = 0.2$, $\mu = 0.1$ and $\sigma = 0.7$ causes homeostatic overload

Combining (9) with (13), we find that

$$y_3^* + rt_1 + rt_2 + r\tau_3 = y_2^* + rt_1 + r\tau_2 \quad (14)$$

$$rt_2 + r\tau_3 - r\tau_2 = y_2^* - y_3^* \quad (15)$$

$$r = \frac{y_2^* - y_3^*}{t_2 - \tau_2 + \tau_3}. \quad (16)$$

We can continue this pattern to find that

$$r = \frac{y_i^* - y_{i+1}^*}{t_i + \tau_{i+1} - \tau_i} \quad (17)$$

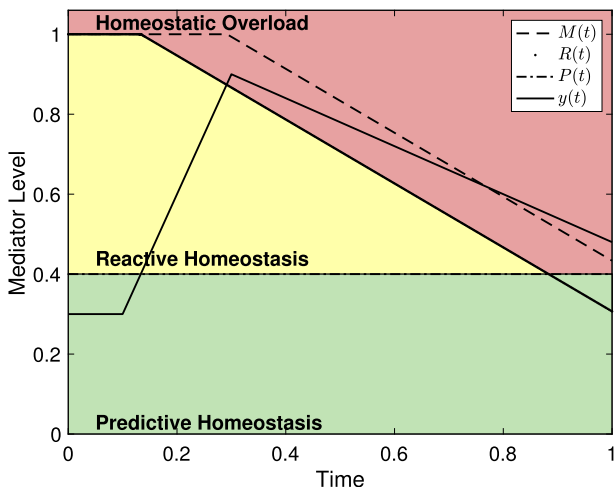


Fig. 10 A physiological mediator whose down-regulation occurs at a lesser rate than r_2 cannot escape homeostatic overload

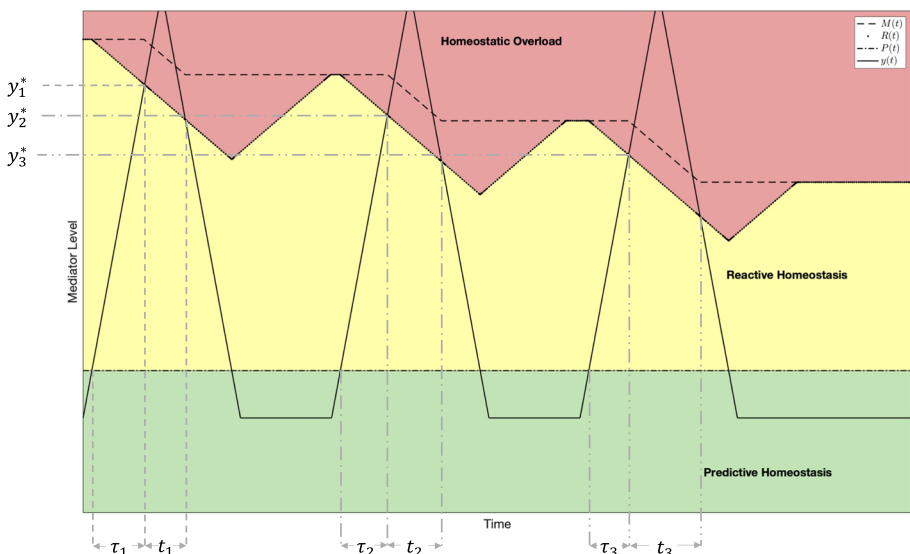


Fig. 11 A graphical depiction of the stress events as described in Sect. 4 with time ranges and corresponding mediator levels labeled. For the purposes of this graph $r_1 = r_2 = r_3 = 2$

meaning that n stress events can be used to compute r a total of $n - 1$ times. Hence, if the value of the ratio given in (17) is consistent across multiple stress events, then the values of the maximal reactive homeostasis and reactive homeostasis must be declining linearly as predicted.

There are several benefits to this approach. First, the actual value of M_0 need not be known. Indeed, since the reactive scope model predicts a decline in $M(t)$ in the event of significant stress, any wild-caught animals are likely to have varying levels

for M_0 . Additionally, any individual animal being examined need only endure three stress responses for a verification and any further stress responses can be used for further verification. Finally, even if the values found are inconsistent, their behavior should indicate how to adjust the decline of reactive scope.

5 Discussion

The mathematical formulation provided in (8) is meant to mimic the description of reactive scope as described by Romero et al. (2009) as much as possible. In this section, we discuss some potential additions to the model as well as weaknesses of the model.

5.1 Potential additions to the model

The reactive scope model as presented in (8) largely describes stress responses in short-term situations. However, an animal's response to stress is likely to change throughout its lifetime (Andrews et al. 2017; Barbi et al. 2018; Haussmann and Heidinger 2015). Senescence may be included in (8) via

$$\begin{aligned}\frac{dM}{dt} &= -r_1\theta(y(t) - R(t)) - A(t) \\ \frac{dR}{dt} &= -r_2\theta(y(t) - P(t)) + r_3\theta(P(t) - y(t))\theta(M(t) - R(t)) - \theta(R(t) - M(t))A(t)\end{aligned}\quad (18)$$

where the function $A(t)$ describes the decline in the maximum threshold for homeostatic overload, $M(t)$, over time. Figure 12 shows two possible examples of (18) using different forms for $A(t)$. As an example, we may define

$$A(t) = \begin{cases} 0 & t \leq a_1 \\ \frac{p_{a_1} - p_{a_2}}{a_1 - a_2} & a_1 < t \leq a_2 \\ 0 & a_2 < t \end{cases}\quad (19)$$

to describe a linear decline between the ages a_1 and a_2 from an $M(t)$ value of p_{a_1} at age a_1 to a value of p_{a_2} at age a_2 . Here, if the time interval in question is an animal's entire lifespan, than $p_{a_1} = M(0)$. An advantage of the form of A given by (19) is that it allows for simple determination of $M(t)$ in the absence of stress events that cause homeostatic overload. That is, if $y(t) < R(t)$ for all t and we incorporate the desired initial conditions, then

$$M(t) = \int \frac{dM}{dt} dt = \int A(t) dt = \begin{cases} M_0 = p_{a_1} & t \leq a_1 \\ \left(\frac{p_{a_1} - p_{a_2}}{a_1 - a_2}\right)(t - a_1) + p_{a_1} & a_1 < t \leq a_2 \\ p_{a_2} & a_2 < t \end{cases}\quad (20)$$

This allows $M(a_1) = p_{a_1} = M_0$ and $M(a_2) = p_{a_2}$. This simplicity allows for the parameters of A to be set once known. However, the form of A given in (19) is not

continuous and describes an abrupt change in the behavior of $M(t)$ and $R(t)$ that may be unrealistic in an animal.

To describe a more natural decline in $M(t)$ and $R(t)$, we may consider $M(t)$ in the absence of stress events with as described by

$$M(t) = p_i - \frac{p_i - p_f}{1 + e^{k(\bar{A}-t)}} \quad (21)$$

where p_i denotes the initial value for $M(t)$, p_f denotes the final value for $M(t)$, k represents the slope of the transition from p_i to p_f , and location parameter \bar{A} represents the midpoint of the transition period from p_i to p_f . For example, if an animal were to live for 100 days, begin its life with $M(0) = M_0$, end its life with $M(t) = 0.6M_0$, with $M(t)$ declining roughly between days 10 and 90 then we would have $p_i = M_0$, $p_f = 0.6M_0$, and $\bar{A} = 90 - 10/2 = 40$. A k value that gives the desired transition rate can be selected. Then we may take

$$A(t) = \frac{d}{dt} \left[p_i - \frac{p_i - p_f}{1 + e^{k(\bar{A}-t)}} \right] = -\frac{k(p_i - p_f)e^{k(\bar{A}-t)}}{\left(1 + e^{k(\bar{A}-t)}\right)^2}. \quad (22)$$

Figure 12 shows $M(t)$ over an animal's lifespan using the two choices for $A(t)$ presented here in the absence of stress events. Since the inclusion of senescence in the reactive scope model requires additional parameters that would require observation over an animal's full lifespan, we leave further discussion of the model with senescence and its verification to future work.

The version of the reactive scope model presented in Sect. 2.2 used the Heaviside function θ to "switch" the behavior of the system provided in (8) based on the mediator value, $y(t)$, in relation to reactive scope threshold, $R(t)$. It might be more appropriate for this switch to happen more gradually as $y(t)$ exceeds $R(t)$. A function that demonstrates this desired behavior is given by

$$\Theta_c(x) = \frac{1}{1 + e^{-cx}} \text{ for } c > 0. \quad (23)$$

As $c \rightarrow \infty$ in (23), the sigmoid function Θ approximates the Heaviside function given by (7). It should be noted that this update would still require the inclusion of the Heaviside function to ensure $R(t) \leq M(t)$. That is, (8) should be updated to

$$\begin{aligned} \frac{dM}{dt} &= -r_1 \Theta_c(y(t) - R(t)) \\ \frac{dR}{dt} &= -r_2 \Theta_c(y(t) - P(t)) + r_3 \Theta_c(P(t) - y(t)) \theta(M(t) - R(t)). \end{aligned} \quad (24)$$

Figure 13 shows the reactive scope model as shown in (24). The only significant change is that the value of $M(t)$ decreases while $y(t) < R(t)$ due to the low choice of $c = 10$ to emphasize this behavior. For a more realistic choice of c (e.g. $c > 20$), the behavior of (24) is nearly indistinguishable from that of (8). Thus, the addition of this

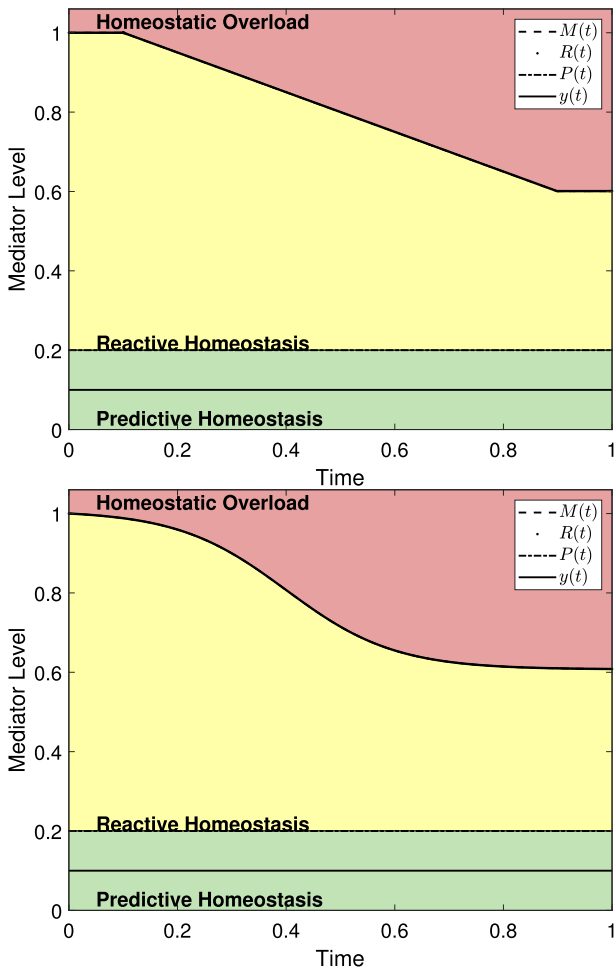


Fig. 12 The reactive scope model shown over an animal's lifetime normalized to $t = 1$ with senescence included and no stress events. (left) The function $A(t)$ as described in (20) is used with $a_1 = 0.1$, $a_2 = 0.9$, $p_{a1} = 1$, and $p_{a2} = 0.6$. (right) The function $A(t)$ as described in (22) is used with $p_i = 1$, $p_f = 0.6$, $\bar{A} = 0.4$, and $k = 10$. Due to the absence of stress, $M(t) = R(t)$ for all t -values and the curves overlap

extra function does little to change the predictions of the model while adding a new parameter that must be estimated in practice. Further, it is possible that the value of c may be different between the two equations in (24). Due to the additional complications introduced by the inclusion of Θ_c in the model, we will not consider it further here but have presented in an effort to consider alternatives.

5.2 Limitations of the reactive scope model

There are limitations to the reactive scope model. There are various physiological mediators at play during any stress response. All such mediators work within their own

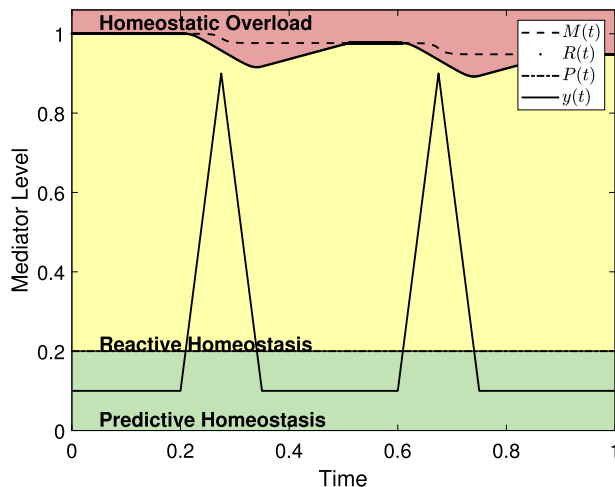


Fig. 13 A demonstration of the reactive scope model using the sigmoid switching function as in (24). Notice that the value of $M(t)$ decreases even though $y(t) < R(t)$ for all t . Here, $r_1 = 2.8$ while $r_2 = r_3 = 0.8$ and $c = -10$ to emphasize the change in $M(t)$

homeostatic ranges and scales and may cause homeostatic overload at different levels (Romero et al. 2015). Thus, should a stress event lead to homeostatic overload, it may not be possible to determine which mediator at play left the reactive homeostasis range and triggered homeostatic overload. There is a growing consensus that glucocorticoids may be an imperfect measure of stress and that measuring more than one mediator is vital to understanding the stress response (Creel et al. 2013; Currie et al. 2010; Du et al. 2009; Jessop et al. 2013; Romero et al. 2015; Tomiyama et al. 2012). After a broad literature review, Dickens and Romero (2013) declared that there is no consensus on the endocrine profile of a chronically stressed wild animal. It was hypothesized by Gormally et al. (2019b) that these variations may be at least partially explained by differences in experimental design pertaining to species and life-history stage.

Further, the values of r_1 , r_2 , and r_3 and even M_0 may be different between various mediators, species, and individuals. As a result, it may be especially challenging to apply experimental results to any wild animal with an unknown life history. However, if general ranges can be established, the reactive scope model may provide valuable insight into wild populations undergoing shared chronic stress like pollution or habitat loss.

The boundary between the predictive homeostatic range and homeostatic range, described as $P(t)$ in (6), represent a potential mathematical challenge since the boundary between reactive homeostasis and homeostatic overload, $R(t)$, only declines when a mediator level exceeds $P(t)$. Thus, determining values for τ as described in Sect. 4 requires being able to determine when this happens empirically. Further, simply capturing a wild-animal and transporting to a lab may be enough to alter the animal's stress physiology (Dickens et al. 2009).

6 Summary

The introduction of the reactive scope model by Romero et al. (2009) provided a novel framework for the study of stress responses in animals. A key feature of this framework is the inclusion of the reactive homeostasis range for mediator levels. Sustained mediator levels within the reactive homeostasis range may cause homeostatic overload via a degradation of the reactive homeostasis range, thereby allowing for a stress event late in an animal's life history (or after other recent stress events) to cause homeostatic overload even when the level of response would not have been enough to cause homeostatic overload early in the animal's life history (or without other recent stress events). To date, the reactive scope model has only been presented as a conceptual model.

Experimental efforts have been made to test the veracity of the reactive scope model (Beattie et al. 2023a; DuRant et al. 2016b, a; Gormally et al. 2019b, a). These experiments have attempted to observe the degradation of the reactive scope range by causing repeated stress events for different groups of wild birds and observing how recovery time between stress events impacts mediator levels in later stress events. Because the reactive scope model existed only as a conceptual model, experimenters could not use the model to determine the necessary duration of stress events to allow for the observation of the degradation of reactive scope, nor the necessary recovery times to allow reactive scope to recover.

We have provided a quantitative formulation of the conceptual reactive scope model. Several possible descriptors (ψ_{μ_i, σ_i}) have been given that can be used to describe the desired curve shapes of mediator levels during stress responses. These descriptors can be combined with information previously collected for a particular mediator in a given species to describe the mediator level as a function of time with the inclusion of stress events ($y(t)$ in (5)). Data already exists that can be used to estimate the parameters needed to accurately describe an animal's mediator levels over times as they fluctuate daily or seasonally. Further, we have captured the dynamic nature of the reactive homeostasis range by providing a system of ordinary differential equations, (8), that describe how the thresholds between the mediator levels change in response to elevated mediator levels. More work must be done before the parameter values in (8) can be estimated. However, such experiments would either provide the necessary estimates or invalidate the current form of the reactive scope model. We have also provided several potential additions or adaptations to the reactive scope model including methods for the incorporation of senescence.

Acknowledgements Funding support was provided by NSF IOS ABR Melding Mathematical and Theoretical Models of Stress grant 1655269.

Declarations

Conflict of interest The authors declare that they have no known competing financial interests or personal relationships that could have appeared to influence the work reported in this paper.

Open Access This article is licensed under a Creative Commons Attribution 4.0 International License, which permits use, sharing, adaptation, distribution and reproduction in any medium or format, as long as you give

appropriate credit to the original author(s) and the source, provide a link to the Creative Commons licence, and indicate if changes were made. The images or other third party material in this article are included in the article's Creative Commons licence, unless indicated otherwise in a credit line to the material. If material is not included in the article's Creative Commons licence and your intended use is not permitted by statutory regulation or exceeds the permitted use, you will need to obtain permission directly from the copyright holder. To view a copy of this licence, visit <http://creativecommons.org/licenses/by/4.0/>.

References

Aguilar RJO, Jahn GA, Soto-Gamboa M, Novaro AJ, Carmanchahi P (2016) The Ecology of Stress: linking life-history traits with physiological control mechanisms in free-living guanacos. *PeerJ* 4:e2640

Andrews C, Nettle D, Larriva M, Gillespie R, Reichert S, Brilot BO, Bateson M (2017) A marker of biological age explains individual variation in the strength of the adult stress response. *R Soc Open Sci* 4(9):171208

Barbi E, Laguna F, Marsili M, Vaupel JW, Wachter KW (2018) The plateau of human mortality: demography of longevity pioneers. *Science (Am Assoc Advance Sci)* 360(6396):1459–1461

Beattie UK, Rosen ES, Fefferman N, Romero LM (2023a) House sparrows prioritize skin repair over constitutive innate immunity during long-term chronic stress. *J Exp Zool A: Ecol Integr Physiol*

Beattie UK, Rosen ES, Fefferman N, Romero LM (2023b) House sparrows prioritize skin repair over constitutive innate immunity during long-term chronic stress. *J Exp Zool A Ecol Integ Physiol*

Breuner CW, Wingfield JC, Romero LM (1999) Diel rhythms of basal and stress-induced corticosterone in a wild, seasonal vertebrate, Gambel's white-crowned sparrow. *J Exp Zool* 284(3):334–342

Cannon W (1932) The Wisdom of the body. W.W. Norton and Company, Inc., New York

Charpentier M, Givalois L, Faurie C, Soghessa O, Simon F, Kappeler P (2018) Seasonal glucocorticoid production correlates with a suite of small-magnitude environmental, demographic, and physiological effects in mandrills. *Am J Phys Anthropol* 165(1):20–33

Creel S, Dantzer B, Goymann W, Rubenstein DR (2013) The ecology of stress: effects of the social environment. *Funct Ecol* 27(1):66–80

Crespi EJ, Williams TD, Jessop TS, Delehanty B (2013) Life history and the ecology of stress: how do glucocorticoid hormones influence life-history variation in animals? *Funct Ecol* 27(1):93–106

Currie S, LeBlanc S, Watters MA, Gilmour KM (2010) Agonistic encounters and cellular angst: social interactions induce heat shock proteins in juvenile salmonid fish. *Proc R Soc B: Biol Sci* 277(1683):905–913

Dempsher DP, Gann DS, Phair RD (1984) A mechanistic model of ACTH-stimulated cortisol secretion. *Am J Physiol Regulat Integ Comp Physiol* 246(4):587–596

Derendorf H, Schmidt S, Rowland M (2020) Rowland and Tozer's clinical pharmacokinetics and pharmacodynamics?: concepts and applications, 5th edn. Wolters Kluwer, Philadelphia

Dickens MJ, Earle KA, Romero LM (2009) Initial transference of wild birds to captivity alters stress physiology. *Gen Comp Endocrinol* 160(1):76–83

Dickens MJ, Romero LM (2013) A consensus endocrine profile for chronically stressed wild animals does not exist. *Gen Comp Endocrinol* 191:177–189

Du J, Wang Y, Hunter R, Wei Y, Blumenthal R, Falke C et al (2009) Dynamic regulation of mitochondrial function by glucocorticoids. *Proc Natl Acad Sci* 106(9):3543–3548

DuRant S, Arciniega M, Bauer C, Romero ML (2016) A test of reactive scope: reducing reactive scope causes delayed wound healing. *Gen Comp Endocrinol* 236:115–120

DuRant S, de Bruijn R, Tran M, Romero L (2016) Wound-healing ability is conserved during periods of chronic stress and costly life history events in a wild-caught bird. *Gen Comp Endocrinol* 229:119–126

Eguizábal GV, Superina M, Palme R, Asencio CJ, Villarreal DP, Borrelli L, Busso JM (2022) Non-invasive assessment of the seasonal stress response to veterinary procedures and transportation of zoo-housed lesser anteater (*Tamandua tetradactyla*). *Animals* 12(1):75

Fawcett TW, Higginson AD (2012) Heavy use of equations impedes communication among biologists. *Proc Natl Acad Sci PNAS* 109(29):11735–11739

Fischer CP, Romero LM (2016) The use of α -or β -blockers to ameliorate the chronic stress of captivity in the house sparrow (*Passer domesticus*). *Conserv Physiol* 4(1)

Gabriel D, Gould L, Cook S (2018) Crowding as a primary source of stress in an endangered fragment-dwelling strepsirrhine primate. *Anim Conserv* 21(1):76–85

Goel N, Workman JL, Lee TT, Innala L, Viau V (2014) Sex differences in the HPA axis. *Compr Physiol* 4(3):1121–1155

Gormally BM, Estrada R, Yin H, Romero LM (2019) Recovery from repeated stressors: physiology and behavior are affected on different timescales in house sparrows. *Gen Comp Endocrinol* 282:113225

Gormally BM, Ramos S, Yin H, Romero LM (2019) Recovery periods during repeated stress impact corticosterone and behavioral responses differently in house sparrows. *Horm Behav* 112:81–88

Grindstaff JL, Beaty LE, Ambardar M, Luttbeg B (2022) Integrating theoretical and empirical approaches for a robust understanding of endocrine flexibility. *J Exp Biol* 225(Suppl_1)

Gudmand-Hoeyer J, Timmermann S, Ottesen JT (2014) Patient-specific modeling of the neuroendocrine HPA-axis and its relation to depression: Ultradian and circadian oscillations. *Math Biosci* 257:23–32

Haussmann MF, Heidinger BJ (2015) Telomere dynamics may link stress exposure and ageing across generations. *Biol Lett* 11(11):20150396

Holmes W, Phillips J (1976) General, comparative and clinical endocrinology of the adrenal cortex [Print]. In: I C-J, H IW (eds) General, comparative and clinical endocrinology of the adrenal cortex. Academic Press, London, pp 293–420

Hosseinichimeh N, Rahmandad H, Wittenborn AK (2015) Modeling the hypothalamus-pituitary-adrenal axis: a review and extension. *Math Biosci* 268:52–65

Houtz JL, Taff CC, Vitousek MN (2022) Gut Microbiome as a Mediator of Stress Resilience: A Reactive Scope Model Framework. *Integr Comp Biol* 62(1):41–57

Howell BR, Sanchez MM (2011) Understanding behavioral effects of early life stress using the reactive scope and allostatic load models. *Dev Psychopathol* 23(4):1001–1016

Jessop TS, Woodford R, Symonds MR (2013) Macrostress: do large-scale ecological patterns exist in the glucocorticoid stress response of vertebrates? *Funct Ecol* 27(1):120–130

Leishman EM, Franke M, Marvin J, McCart D, Bradford C, Gyimesi ZS et al (2022) The adrenal cortisol response to increasing ambient temperature in polar bears (*Ursus maritimus*). *Animals* 12(6):672

Levine S (2005) Handbook of stress and the brain. In: Steckler T, Kalin NH, Reul JHM (eds) Handbook of stress and the brain, 1st edn. Elsevier, Amsterdam, pp 3–23

Lightman SL (2008) The neuroendocrinology of stress: a never ending story. *J Neuroendocrinol* 20(6):880–884

Lightman SL, Conway-Campbell BL (2010) The crucial role of pulsatile activity of the HPA axis for continuous dynamic equilibration. *Nat Rev Neurosci* 11(10):710–718

Lima AS, de Figueiredo AC, Floreste FR, Garcia Neto PG, Gomes FR, Titon SCM (2022) Temperature extreme events decrease endocrine and immune reactive scope in Bullfrogs (*Lithobates catesbeianus*). *Integr Comp Biol* 62(6):1671–1682

Luttbeg B, Beaty LE, Ambardar M, Grindstaff JL (2021) Mathematical modeling reveals how the speed of endocrine regulation should affect baseline and stress-induced glucocorticoid levels. *Horm Behav* 136:105059

McEwen BS (1998) Protective and damaging effects of stress mediators. *N Engl J Med* 338(3):171–179

McEwen BS (2003) Interacting mediators of allostasis and allostatic load: towards an understanding of resilience in aging. *Metab Clin Exp* 52(10 Suppl 2):10–16

McEwen BS, Wingfield JC (2003) The concept of allostasis in biology and biomedicine. *Horm Behav* 43(1):2–15

Moore-Ede MC (1986) Physiology of the circadian timing system: predictive versus reactive homeostasis. *Am J Physiol Regulat Integ Comp Phys* 250(5):737–752

Nicolaides NC, Charmandari E, Kino T, Chrousos GP (2017) Stress-related and circadian secretion and target tissue actions of glucocorticoids: impact on health. *Front Endocrinol (Lausanne)* 8:70

Pahuja HK, Narayan EJ (2021) Reactive scope model and emergency life history stage provide useful tools for evaluating the stress responses of native Australian lizards living in disturbed landscapes. *Conserv Physiol* 9(1):coab097

Rao R, Androulakis IP (2019) Allostatic adaptation and personalized physiological trade-offs in the circadian regulation of the HPA axis: A mathematical modeling approach. *Sci Rep* 9(1):11212–11215

Rich EL, Romero LM (2005) Exposure to chronic stress downregulates corticosterone responses to acute stressors. *Am J Physiol Regulat Integ Comp Physiol* 288(6):1628–1636

Roast MJ, Aulsebrook AE, Fan M, Hidalgo Aranzamendi N, Teunissen N, Peters A (2019) Short-term climate variation drives baseline innate immune function and stress in a tropical bird: a reactive scope perspective. *Physiol Biochem Zool* 92(2):140–151

Romero LM (2012) Using the reactive scope model to understand why stress physiology predicts survival during starvation in Galápagos marine iguanas. *Gen Comp Endocrinol* 176(3):296–299

Romero LM, Dickens MJ, Cyr NE (2009) The reactive scope model – A new model integrating homeostasis, allostasis, and stress. *Horm Behav* 55(3):375–389

Romero LM, Platts SH, Schoech SJ, Wada H, Crespi E, Martin LB, Buck CL (2015) Understanding stress in the healthy animal—potential paths for progress. *Stress* 18:491–497. <https://doi.org/10.3109/10253890.2015.1073255>

Schoenle LA, Zimmer C, Vitousek MN (2018) Understanding context dependence in glucocorticoid-fitness relationships: the role of the nature of the challenge, the intensity and frequency of stressors, and life history. *Understanding context dependence in glucocorticoid-fitness relationships: the role of the nature of the challenge, the intensity and frequency of stressors, and life history. Integr Comp Biol* 58(4):777–789

Selye H (1946) The general adaption syndrom and the diseases of adaption. *The general adaption syndrom and the diseases of adaption. J Clin Endocrinol* 6:117–230

Servedio MR, Brandvain Y, Dhole S, Fitzpatrick CL, Goldberg EE, Stern CA, Yeh DJ (2014) Not just a theory—the utility of mathematical models in evolutionary biology. *PLoS Biol* 12(12):e1002017

Spiga F, Walker JJ, Gupta R, Terry JR, Lightman SL (2015) 60 YEARS OF NEUROENDOCRINOLOGY: Glucocorticoid dynamics: insights from mathematical, experimental and clinical studies. *J Endocrinol* 226(2):T55–T66

Stanojević A, Marković VM, Čupić V, Kolar-Anić L, Vukojević V (2018) Advances in mathematical modelling of the hypothalamic-pituitary-adrenal (HPA) axis dynamics and the neuroendocrine response to stress. *Curr Opin Chem Eng* 21:84–95

Sterling P, Eyer J (1988) Handbook of Life stress cognition and health. In: Fisher S, Reason J (eds) Wiley, New York, pp 629–650

Taborsky B, English S, Fawcett TW, Kuijper B, Leimar O, McNamara JM, Sandi C (2021) Towards an evolutionary theory of stress responses. *Trends Ecol Evol* (Amsterdam) 36(1):39–48

Taborsky B, Kuijper B, Fawcett TW, English S, Leimar O, McNamara JM, Ruuskanen S (2022) An evolutionary perspective on stress responses, damage and repair. *An evolutionary perspective on stress responses, damage and repair. Horm Behav* 142:105180

Tomiyama AJ, O'Donovan A, Lin J, Puterman E, Lazaro A, Chan J et al (2012) Does cellular aging relate to patterns of allostasis? An examination of basal and stress reactive HPA axis activity and telomere length. *Physiol Behav* 106(1):40–45

Tsigos C, Chrousos GP (2002) Hypothalamic-pituitary-adrenal axis, neuroendocrine factors and stress. *J Psychosom Res* 53(4):865–871

Vinther F, Andersen M, Ottesen JT (2011) The minimal model of the hypothalamic-pituitary-adrenal axis. *J Math Biol* 63(4):663–690

Zavala E, Wedgwood KC, Voliotis M, Tabak J, Spiga F, Lightman SL, Tsaneva-Atanasova K (2019) Mathematical Modelling of Endocrine Systems. *Trends Endocrinol Metab* 30(4):244–257

Publisher's Note Springer Nature remains neutral with regard to jurisdictional claims in published maps and institutional affiliations.

Authors and Affiliations

Justin Wright^{1,2}  · Kelly Buch³ · Ursula K. Beattie⁴ ·
Brenna M. G. Gormally⁴ · L. Michael Romero⁴ · Nina Fefferman^{1,2}

Kelly Buch
buchk@apsu.edu

Ursula K. Beattie
Ursula.Beattie@tufts.edu

Brenna M. G. Gormally
bgormally@ucsd.edu

L. Michael Romero
michael.romero@tufts.edu

Nina Fefferman
nfefferm@utk.edu

- ¹ Department of Ecology and Evolutionary Biology, University of Tennessee Knoxville, 569 Dabney, Knoxville 37996, TN, USA
- ² National Institute of Mathematical and Biological Synthesis, Knoxville, TN 37996, USA
- ³ Department of Mathematics and Statistics, Austin Peay State University, Maynard Mathematics and Computer Science Building Room 205, Clarksville, TN 37044, USA
- ⁴ Department of Biology, Tufts University, 200 Boston Ave #4700, Medford, MA 02155, USA